Cellular Physiology and Biochemistry

Cell Physiol Biochem 2018;47:1682-1695

DOI: 10.1159/000490986
Published online: June 27, 2018

Accepted: February 02, 2018

© 2018 The Author(s)
Published by S. Karger AG, Basel
www.karger.com/cpb

This article is licensed under the Creative Commons Attribution-NonCommercial-NoDerivatives 4.0 International License (CC BY-NC-ND) (http://www.karger.com/Services/OpenAccessLicense). Usage and distribution for commercial purposes as well as any distribution of modified material requires written permission.

Original Paper

MicroRNA-142 Inhibits Proliferation and Promotes Apoptosis in Airway Smooth Muscle Cells During Airway Remodeling in Asthmatic Rats via the Inhibition of TGF-β -Dependent EGFR Signaling Pathway

Jing Wang[a] Hu-Shan Wang[b] Zhen-Bo Su[c]

[a]Respiratory Department, China-Japan Union Hospital of Jilin University, Changchun, [b]Department of Anesthesiology, The First Hospital of Jilin University, Changchun, [c]Department of Anesthesiology, China-Japan Union Hospital of Jilin University, Changchun, P.R. China

Key Words
MicroRNA-142 • Transforming growth factor-β • EGFR signaling pathway • Asthma • Airway remodeling • Airway smooth muscle cells • Proliferation • Apoptosis

Abstract
Background/Aims: Asthma is a heterogeneous disease characterized by chronic airway inflammation resulting from airway hyper-responsiveness to diverse stimuli. In this study, we investigated whether microRNA-142 (miR-142) expression affects proliferation and apoptosis in airway smooth muscle cells (ASMCs) during airway remodeling in asthmatic rats. ***Methods:*** Thirty six Wistar rats were randomly classified into a control group and an model group. miR-142 mimics and inhibitors were constructed, and ASMCs were transfected using liposomes according to the following groups: blank, negative control (NC), miR-142 mimics, miR-142 inhibitors, si-TGF-β and miR-142 inhibitors + si-TGF-β. We verified that miR-142 targets TGF-β using a dual-luciferase reporter assay. The expression levels of miR-142, TGF-β, EGFR and apoptosis signaling pathway-related genes were determined using RT-qPCR and western blotting. Changes in cell proliferation, cell cycle progression and apoptosis were analyzed using MTT assays and flow cytometry. ***Results:*** Rats with asthma had higher expression levels of EGFR and Akt and lower miR-142 levels. miR-142 was negatively correlated with TGF-β expression. In ASMCs, the expression of TGF-β, EGFR, Akt, phosphorylated-Akt (p-Akt), Bcl-2 and Bcl-xl and the rate of early apoptosis were decreased while expression of Bax and p21 and the proliferation rate were elevated with the upregulation of miR-142. The opposite results were observed with the downregulation of miR-142. Finally, the proliferative rate was decreased while the apoptosis rate was increased and expression levels of EGFR, Akt, p-Akt, Bcl-2 and Bcl-xl were reduced while Bax and p21 were elevated in the ASMCs transfected with miR-142 inhibitors and si-TGF-β. ***Conclusion:*** The results of our study suggest that miR-142

Dr. Zhen-Bo Su

Department of Anesthesiology, China-Japan Union Hospital of Jilin University,
No. 126 Xiantai Street, Changchun 130033, Jilin Province, (China)
Tel. +86-0431-89876551, E-Mail suzb@jlu.edu.cn

inhibits proliferation and promotes apoptosis in ASMCs during airway remodeling in asthmatic rats by inhibiting TGF-β expression via a mechanism involving the EGFR signaling pathway.

© 2018 The Author(s)
Published by S. Karger AG, Basel

Introduction

Asthma is a chronic inflammatory airway disorder characterized by reversible airflow obstruction and airway hyper-responsiveness [1]. Many types of inflammatory cells play roles in asthma by releasing inflammatory mediators that cause sustained chronic inflammation of the airways. This triggers bronchoconstriction and airway structural changes [2], the latter of which initially serves as a repair process initiated in response to inflammation-induced injury to the airway wall. However, dysregulation of this repair process leads to airway remodeling [3]. Airway remodeling induces pathophysiologic modifications in normal airway wall structures, including changes in the organization and composition of the airway wall's molecular and cellular components [4]. These changes are strongly suspected to lead to physiologic subphenotypes, such as irreversible or partially reversible airflow obstruction and decreased lung function [5]. With increased proliferation and migration of airway smooth muscle cells (ASMCs), the airway smooth muscle (ASM) thickens, leading to the remodeling of airway wall smooth muscles [6]. The prevalence of asthma markedly increased during the second half of the last century, and asthma is currently a considerable disease burden for individuals and a substantial economic burden on society and healthcare systems [7]. Therefore, developing new therapeutic strategies to reverse airway remodeling and thereby combat asthma is of paramount importance, and identifying the mechanisms responsible for airway remodeling will support this goal [5].

MicroRNAs (miRNAs) are a large family of post-transcriptional gene expression regulators ~21 nucleotides in length that control many cellular and developmental processes in eukaryotic organisms [8]. miR-142 is a global inhibitor of cytokine signaling. Preventing the physiological downregulation of miR-142 has been shown to induce apoptosis and deplete cytokine-mediated survival signals [9]. The transforming growth factor-β (TGF-β) family includes several TGF-β isoforms (e.g., TGF-β1, TGF-β2, and TGF-β3) in addition to inhibins, activins, differentiation factors and growth factors; the diverse roles of TGF-β family members include regulation of immune responses, chemotaxis for inflammatory cells, and proliferation inhibition of many cell types [2]. miR-142-5p is capable of negatively regulating the TGF-β pathway by targeting SMAD3, and according to functional studies, hsa-miR-142-5p plays a role in TGFβ signaling by inhibiting TGFβ receptor 2 [10, 11]. In addition, miR-142-3p can modulate ASMC phenotypes via a TGF-β-mediated mechanism [12]. One study suggested a close correlation between the activation of the TGF-β pathway and the pathogenesis underlying asthma-induced airway remodeling [13]. Epidermal growth factor receptor (EGFR) activation plays an essential role in the migration, differentiation and proliferation of numerous human epithelial cell types [14]. Epithelial EGFR expression was found to be increased in damaged airways of asthmatic patients [15], suggesting that the EGFR signaling pathway may be modulated in asthmatic airways. Therefore, this study sought to explore the functions and mechanisms by which miR-142, TGF-β and EGFR regulate proliferation and apoptosis of ASMCs during airway remodeling in asthmatic rats, with the ultimate aim of identifying new therapeutic targets.

Materials and Methods

Ethics statement

All the animal experiments were approved by the ethics committee of China-Japan Union Hospital of Jilin University.

Study subjects

This study included 36 male Wistar rats of specific-pathogen free (SPF) grade weighing 292 g to 345 g (Hunan SJA Laboratory Animal Co., Ltd., Chanagsha, China). Feeding, water supply, light, and temperature were maintained at consistent levels, and all the animals were housed under SPF conditions. Environmental conditions in the facilities were consistent with the relevant guidelines of the Chinese national standard "Laboratory animal-requirements of environment and housing facilities" (GB14925-2001) for experimental animal barrier facilities.

Animal groups and treatments

Thirty six Wistar rats were randomly classified into a control group (n = 18) and an model group (n = 18). The rats were submitted to one week of adaptive feeding. On the first day following adaptation, the rats were given 1 ml of normal saline containing 100 mg ovalbumin (OVA; Shanghai Sangon Biotech Co., Ltd., Shanghai, China) and 200 mg aluminum hydroxide (Beijing Solarbio Science & Technology Co., Ltd, Beijing, China) by subcutaneous hind leg injection, with 1 ml of pertussis vaccine (approximately 6 ×109 strains; Beijing Bitab Biotechnology Co., Ltd., Beijing, China) given by intraperitoneal injection as an adjuvant. A repeat sensitization protocol was performed once on day 8, and exposure was initiated on the day 15. The rats were placed in a special glass container, and 50 ml 2% OVA in normal saline was injected into the container using ultrasonic nebulization. The rats were exposed to this treatment for 30 min at 3 times per week for 6 consecutive weeks. The control group received normal saline alone. The rats were sacrificed within 24 h following the last exposure period. Trachea, bronchus and lung tissues were isolated, and the right middle lung was removed after ligation. Lung specimens were preserved in 4% paraformaldehyde and then subjected to conventional paraffin embedding, sectioning and hematoxylin-eosin (HE) staining. Airway pathology was evaluated under a microscope.

Pathological image analysis

A complete lung cross section was imaged by microscope, and image analysis software was used to measure the internal perimeter (Pi), area (WA), and external perimeter (Pe) of the lung wall, bronchial smooth muscle area (S) and the number of bronchial smooth muscle cell nuclei (N). The three measured values were normalized using Pi and S and are expressed as WA/Pi2, S/Pi2, and N/S.

Quantitative reverse transcription polymerase chain reaction (RT-qPCR)

Total RNA was extracted from cells and tissues using the TRIzol 1-step method (Invitrogen Inc., Carlsbad, CA, USA). A small volume of liquid nitrogen was used to grind the tissues to a uniform powder, and Trizol reagent was then added to extract RNA. Diethylpyrocarbonate (DEPC)-treated ultra-pure water was applied to the mixture to dissolve the RNA. An ND-1000 UV-Visible Spectrophotometer (Nanodrop, Wilmington, DE, USA) was used to measure optical density (OD) at 260 nm and 280 nm. The quality of the total RNA was determined, and RNA concentration was adjusted accordingly. The extracted RNA was reverse-transcribed using a two-step method according to the manufacturer's instructions (Fermentas Inc., Hanover, MD, USA). The following reaction conditions were used: 70°C for 10 min, ice-bath for 2 min, 42°C for 60 min and 70°C for 10 min. The reverse-transcribed cDNA was temporarily placed at -80°C. RT-qPCR was conducted using the TaqMan probe method. according to the manufacturer's instructions (Fermentas Inc., Hanover, MD, USA). The primer sequences are shown in Table 1, and the reaction conditions were as follows: one cycle of pre-denaturation at 95°C for 30 s followed by 40 cycles of denaturation at 95°C for 10 s, annealing at 60°C for 20 s, and extension at 70°C for 10 s. An RT-qPCR platform (Bio-Rad iQ5, Bio-Rad, Inc., Hercules, CA, USA) was used for detection. U6 was used as an internal reference for miR-142, and β-actin was used for other target genes. Using the

Table 1. Primer sequences of related genes for RT-qPCR. Notes: miR-142, microRNA-142; TGF-β, transforming growth factor-β; EGFR, epidermal growth factor receptor; RT-qPCR, reverse transcription quantitative polymerase chain reaction

Target genes	Primer Sequences
miR-142	Forward 5'-GTCACCTGTAGTGTTTCCTACTT-3' Reverse 5'-TATGGTTGTTCTGCTCTCTGTCTC-3'
U6	Forward 5'-ATTGGAACGATACAGAGAAGATT -3' Reverse 5'-GGAACGCTTCACGAATTTG -3'
TGF-β	Forward 5'-ACTGATACGCCTGAGTGGCTGT-3' Reverse 5'-CTCTGTGGAGCTGAAGCAGTAG-3'
EGFR	Forward 5'-ACC GGC AGG ATG TGG AGA TC -3' Reverse 5'-GGC CGA CAG CTA TGA GAT CCA -3'
Akt	Forward 5'--GGGCTAGCGATGAGCGACGTGGCTATTGTG-3' Reverse 5'-GGGGTACCGGCCGTGCCGCTGGCCGAGTAG-3'
β-actin	Forward 5'-CGTGCGTGACATTAAAGAG-3' Reverse 5'-TTGCCGATAGTGATGACCT -3'

relative quantitative method, the relative expression multiple of each target gene was expressed as 2-ΔΔCt. Each experiment was repeated 3 times.

Western blotting

Total protein samples were obtained from cells and tissues and added to a 1X sodium dodecyl sulfate (SDS) lysis solution. Next, the protein extract was heated to 100°C for 5 min. A bicinchoninic acid (BCA) assay was used for protein quantification. The samples were adjusted to the same concentration (1 μg/μl) using deionized water. Then, 20 μg of sample was loaded and electrophoresed on a 12% polyacrylamide gel. After transferring the blots to nitrocellulose membranes, the samples were blocked for 1 h at room temperature on a decolorization table in Tris-buffered saline-Tween (TBS-T) containing 5% bovine serum albumin (BSA). The blocking solution was then discarded, and the membrane was placed into a plastic groove. Membranes were incubated with antibodies against TGF-β, EGFR, p-EGFR, Akt, p-Akt, Bax, Bcl-2, Bcl-xl, p21 and β-actin (Cell Signaling Technologies, Beverly, MA, USA) in 5% BSA with the transfer surface facing upward and placed in a refrigerator overnight at 4°C with shaking. The next day, the membranes were rinsed in TBS-T (3 times × 10 min each). The diluted secondary antibody (Abcam, Cambridge, Inc., MA, USA) was added to the membrane. After 4-6 h, the membrane was washed with TBS-T (3 times × 15 min each). Chemiluminescence reagent A solution and B solution were mixed at a ratio of 1:1, and the mixture was dripped uniformly onto the membranes. The membranes were developed, and all immunoblot bands were subjected to relative densitometric analysis.

Cultivation and identification of ASMCs

According to the reference method [16], rats in the model group were anesthetized, and their lungs were removed and place in pre-chilled D-Hank's solution. The main bronchus was cleaned three times and separated. Airways with an internal diameter of 2-3 mm without cartilage were selected. The bronchus was stripped under a dissecting microscope, and the airway intima was removed using a sharp tool. Then, the resulting single layer of smooth muscle was cut into small sections of approximately 1 mm3. Approximately 1 mg/ml of type I collagenase and 1 mg/ml of papaya protease (Gibco Company, Grand Island, NY, USA) were added, and the muscle was digested for 30 min at 37°C. Next, Dulbecco's minimum essential medium (DMEM) containing 20% fetal bovine serum (FBS) was added to the mixture to terminate digestion. The mixture was then centrifuged for 10 min at 1000 RPM. The supernatant was then discarded, and the precipitate was extracted. The mixture was added to DMEM culture medium containing 20% FBS (including 20 u/ml penicillin and 20 u/ml streptomycin), and the resulting solution was inoculated in a 25 ml culture flask and cultured at 37°C in a 5% CO_2 incubator. The medium was changed once every 2-3 d, and cells began to grow after 3-5 d. Once primary cells covered the culture flask, 0.25% trypsin was used to digest and passage the cells. The culture medium was replaced with DMEM containing 10% FBS. Cell morphology was analyzed using immunofluorescence and immunohistochemistry assays with anti-smooth muscle actin (α-actin) antibodies. Cells from passages 3 to 5 were selected for these experiments.

Dual-luciferase reporter gene assay

The biological prediction website microRNA.org was used to guide the analysis of miR-142 target genes. This website was used to predict genes that are potentially targeted by miR-142 and identify potential target sites. DNA was extracted from ASMCs obtained from rats in the control group. This procedure was performed in strict accordance with the manufacturer's instructions using the TIANamp Genomic DNA Kit (Tiangen Biotech, Beijing, China). A TGF-β 3'UTR wild-type sequence (TGF-β -3'-UTR-wt) and a TGF-β 3'UTR sequence in which the miRNA-142 binding site was deleted (TGF-β-3'-UTR-mut) were designed as follows: TGF-β-3'-UTR-wt, forward 5'-TTCCTCGAGGCTGCCCCGGGTCCCCA-3' and reverse 5'-TGCGCGGCCGCTCAGGCTTTGAAAAACAAACCC-3'; and TGF-β-3'-UTR-mut, forward 5'-CAGAAATAATCTGCTTATCAGGCAA-3' and reverse 5'-TTGCCTGATAAGGCAGATTATTTCTG-3'. A luciferase reporter vector was constructed and transfected into ASMCs. Luciferase activity assays were performed using a luciferase reporter gene assay kit (Promega Corporation, Madison, WI, USA). Forty-eight hours post-transfection, the culture medium was removed, and the cells were washed two times with phosphate-buffered saline (PBS). Next, 100 μl of passive lysis buffer (PLB) was added to each well, and the plates were gently shaken for 15 min at room temperature. Cell lysate was then collected. The program was set for a pre-reading time of 2 s and a reading time of 10 s. Each sample volume of LARIIStop&Glo® Reagent contained

100 μl. The formulated LARIIStop&Glo® Reagent was added to a luminous tube containing cell lysate (20 μl per sample), and the tube was then placed in a bioluminescence detector (Modulus™, Turner BioSystems company CA, USA).

Cell groups and transfection

The cells were assigned to a blank group (ASM from the model group, mock transfection), a negative control (NC) group (ASM from the model group transfected with the negative control sequence 5'-UCAACAUCAGUCUGAUAAGCUA-3'), an miR-142 mimics group (ASM from the model group transfected with the miR-142 mimic 5'-GACAGUGCAGUCACCCAUAAAG UAGAAAGCACUACUAACAGCACUGGAGGGUGUA GUGUUUCCUACUUUAUGGAUGAGUGUACUGUG-3'), an miR-142 inhibitors group (ASM from the model group transfected with the miR-142 inhibitor 5'- CACAGUACACUCAUCCAUAA AGUAGGAAACACUACACCCUCCAGUGCUGUUUUA GUAGUGCUUUCUACUUUAUGGGUGACUGCACUGUC-3'), an inhibitors + si-TGF-β group (ASM from the model group transfected with miR-142 inhibitors + si-TGF-β interference sequence), and an si-TGF-β group (ASM from the model group transfected with si-TGF-β interference sequence). The miRNA-142 inhibitors and si-TGF-β were purchased from Sangon Biotech, Co. Ltd., Shanghai, China, and Shanghai Genechem Co., Ltd., Shanghai, China, respectively. After being seeded in 25 cm2 flasks, the cells were grown to 30~50% density in complete culture medium. Then, 5 μl of Lipofectamine 2000 (Invitrogen Inc., Carlsbad, CA, USA) was diluted in 100 μl of serum-free medium in a sterile Eppendorf (EP) tube and incubated for 5 min at room temperature. Next, 1 μg of DNA was added to the mixture, and the solution was gently and evenly mixed and incubated for 20 min at room temperature to allow the DNA and liposomes to form complexes. The cells grown in the culture flasks were washed in serum-free medium. Then, serum-free medium was added to the complex (without antibiotics), the solution was mixed gently and placed in a culture flask for transfection. The flask was incubated in 5% CO_2 at 37°C. After 6-8 h, the medium was replaced, and fresh complete medium was added to the cells. Transfection efficiency was evaluated under a fluorescence microscope at 24 h post-transfection. A single-cell suspension was prepared using 0.25% trypsin. Then, PBS was added to the cell suspension, and the mixture was centrifuged at 800 g for 5 min. The supernatant was discarded, and the mixture was rinsed twice with PBS. Cell concentration was adjusted to 1 × 106 cells/ml, and a machine inspection was performed. Untransfected cells were used as a negative control. When the efficiency was found to be greater than 90%, subsequent experiments were performed.

MTT assay

When the growth density of the transfected cells reached 80%, the cells were washed twice with PBS and digested using 0.25% trypsin to prepare single cell suspensions. After counting, the cells were inoculated into 96-well plates (3×10^3 - 6×10^3 cells per well in 200 μl). In total, there were 6 replicates for each group. Next, 5 mg/ml MTT solution (20 μl, Sigma Aldrich, St. Louis, MO, USA) was added to each well. After the cells were incubated for 4 h in an incubator, the culture medium was discarded. Approximately 150 μl dimethyl sulfoxide (DMSO; Sigma Aldrich, St. Louis, MO, USA) was added, and the solution was gently shaken for 10 min. The optical density (OD) value of each well was determined using an enzyme-linked immunosorbent assay (ELISA) at a wavelength of 490 nm at 24 h, 48 h, and 72 h. A cell viability curve was constructed with time points used as the x-axis and OD values as the y-axis.

Flow cytometry

For cell cycle analysis, cells were collected 48 h post-transfection and washed 3 times with cold PBS. The cells were centrifuged, the supernatant discarded, and the cell concentration was adjusted to 1×10^5 cells/ml. Next, the cells were fixed using 1 ml of 75% cold ethanol at 4°C overnight and then washed twice with PBS. Cells were washed twice with PBS and the supernatants were discarded before staining. RNase A (100 μl) was added, and the mixture was incubated for 30 min in a 37°C water bath in the dark. Next, 400 μl of propidium iodide (PI) (Sigma Aldrich, St. Louis, MO, USA) was added, and the solution was mixed and allowed to rest for 30 min at 4°C in the dark. Flow cytometry (Becton Dickinson Bio-sciences, San Jose, CA, USA, FACSCanto II) was then used for cell cycle detection at an excitation wavelength of 488 nm.

Double staining with Annexin-V and PI was used to analyze apoptosis. At 48 h after transfection, the cells were collected in a flow tube and centrifuged for 5 min at 1000 r/min. The supernatant was then discarded. The cells were washed 3 times with cold PBS and then centrifuged, and the supernatants were discarded.

According to the instructions included with the Annexin-V-FITC cell apoptosis assay kit (Sigma Aldrich, St. Louis, MO, USA), 150 μl of binding buffer and 5 μl of Annexin-V-FITC were added to each cell solution, and the solutions were mixed well. Next, the cells were incubated for 15 min at room temperature in the dark, and 100 μl of binding buffer and 5 μl of PI stain (Sigma Aldrich, St. Louis, MO, USA) were then added. The solution was oscillated and mixed, and the rate of apoptosis was determined using flow cytometry.

Statistical analysis

All the data were analyzed using SPSS 21.0 (IBM Corp. Armonk, NY, USA) statistical software. Measurement data with a normal distribution are expressed as the mean ± standard deviation (SD). One-way analysis of variance was used for comparisons among multiple groups. Comparisons between two groups were analyzed using t-tests and correlation analyses using Pearson's correlation method. $P < 0.05$ indicates statistical significance.

Results

Pathological changes are observed in the airway wall structures of rats in the model groups

HE staining was conducted to observe the pathological changes of rats. All the rats in the model group showed symptoms including irritability, cough, frequent scratching, shortness of breath, irregular rhythm and mild cyanosis after each OVA exposure. After the rats had been continuously exposed for several days, the reaction was slower in the model group rats compared with that in the normal group. The color of the rats' fur also became dull. In rat lung tissue sections, H&E staining showed blue-black nuclei and pale red cytoplasm (Fig. 1). The model group exhibited more bronchial mucosal folding and fractures, large-scale infiltration of eosinophils in the submucosa and tube wall, a mucus plugging in the lumen, and thicker and more uneven airway walls and ASMs. No pathological changes were observed in the airway wall structures of the control group. The image analysis results (Table 2) showed that the bronchial wall thickness (WA/Pi2), the smooth muscle thickness of the bronchial wall (S/Pi2), and the number of smooth muscle cells in the bronchial wall (N/S) were significantly higher in the model group than those in the control group (all $P < 0.05$). These values were increased by 42.5%, 58.7% and 50.0%, respectively. These abovementioned results suggested that the pathological changes are observed in the airway wall structures of rats in the experimental groups.

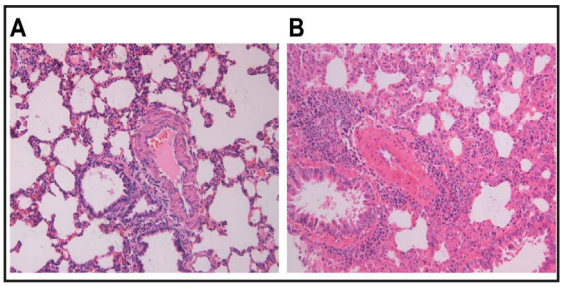

Fig. 1. Airway pathology in the normal group and model group. Notes: A, normal group; B, model group.

Group	WA/Pi (μm2/μm2)	S/Pi (μm2/μm2)	N/Pi (per/μm2)
Normal group	3.51 ± 0.95	1.30 ± 0.42	0.06 ± 0.01
Model group	6.64 ± 0.88*	2.75 ± 0.56*	0.09 ± 0.01*

Table 2. Comparisons of WA/Pi, S/Pi2, N/S between the normal group and asthma group. Notes: *, $P < 0.05$ compared with the normal group; n = 18.

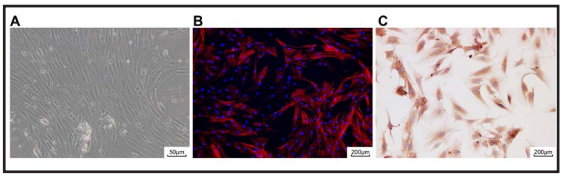

Fig. 2. Cell type identification in ASMCs in rats with asthma.Notes: A, In vitro cultures of ASMCs obtained from rats with asthma. The cells were analyzed under a normal optical microscope (× 100). B, Immunofluorescence diagram of ASMCs obtained from rats with asthma (× 400). Red fluorescence in the intracytoplasmic compartment indicates that staining for α-actin was positive, while blue fluorescence in the nucleus indicates that nuclear staining was positive. C, Immunofluorescence diagram of in vitro cultures of ASMCs obtained from rats with asthma (× 400). The brown-yellow granules in the cytoplasm represent cells that were positive for α-actin staining; n = 3. A total of 5 fields of vision were selected from an image obtained from each rat.

Identification of ASMCs in the rats with asthma

An analysis of ASMCs (Fig. 2) performed under an inverted microscope showed that single cells were spindle shaped, had a long protuberance, contained abundant cytoplasm and possessed round nuclei located in the center of the cell. When the cell density reached a high level, the cells partially overlapped, resulting in a "peak and valley" morphology. Under fluorescence imaging, red fluorescence indicated that the cells were positive for α-actin staining. The cells also showed positive blue fluorescence, indicating that they possessed nuclei. The immunohistochemistry results showed that brown-yellow granules observed in the cytoplasm were positive for α-actin staining. All the cells staining positive for nuclei were also found to be positive for α-actin staining in the cytoplasm, suggesting that the cultured cells were ASMCs.

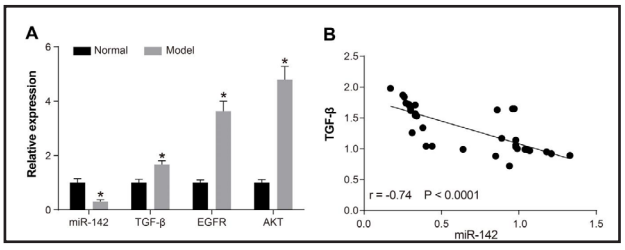

Fig. 3. Expression of miR-142 and the mRNA expression levels of TGF-β and EGFR signaling pathway-related genes in the normal and model groups as well as an analysis of the correlation between miR-142 and TGF-β. Notes: A, Expression of miR-142 and the mRNA expression levels of TGF-β and EGFR signaling pathway-related genes between the normal and model groups. B, Correlation analysis of miR-142 and TGF-β; *, compared to the normal group, P<0.05; n = 18 in each group; the experiment was repeated 3 times; miR-142, microRNA-142; TGF-β, transforming growth factor-β; EGFR, epidermal growth factor receptor.

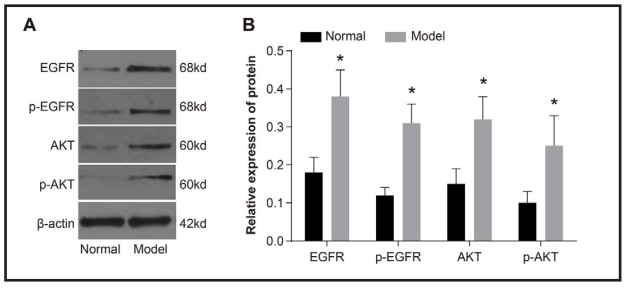

Fig. 4. Expression levels of EGFR signaling pathway-related proteins in rat ASMCs in the normal and model groupsNotes: A, protein expression levels of EGFR, p-EGFR, Akt and p-Akt as determined using western blotting; B, histogram analysis of the protein expression levels of EGFR, p-EGFR, Akt and p-Akt; *, compared to the normal group, P<0.05; n = 18 in each group; the experiment was repeated 3 times; ASMCs, airway smooth muscle cells; EGFR, epidermal growth factor receptor.

Lower expression levels of miR-142, and higher expression levels of TGF-β and EGFR signaling pathway-related genes are found in the rats with asthma

ASMCs were analyzed from the rats in each group by RT-qPCR. The results (Fig. 3A) showed that miR-142 was expressed at significantly lower levels while TGF-β and the EGFR pathway-related genes EGFR and Akt were expressed at markedly higher levels in ASMCs from the model group than those in the control group (all P < 0.05). Pearson's analysis showed a negative correlation between miR-142 and mRNA levels of TGF-β (r = - 0.74 and P < 0.05) (Fig. 3B). It can be concluded that lower expression level of miR-142, and higher expression levels of TGF-β and EGFR signaling pathway-related genes are found in rats with asthma. Expressions of EGFR signaling pathway-related proteins are higher in ASMCs from the rats with asthma. Next, the expression of EGFR signaling pathway-related proteins in ASMCs obtained from rats with asthma was also detected. Western blot analyses of rat ASMCs (Fig. 4) showed that protein levels of EGFR, phosphorylated-EGFR (p-EGFR), Akt and phosphorylated-Akt (p-Akt) were significantly higher in the model group than those in the control group (all P < 0.05). It suggested that Expressions of EGFR signaling pathway-related proteins are higher in ASMCs obtained from rats with asthma.

TGF-β is a target gene of miR-142

The online prediction software at microRNA.org was used to identify the miR-142 binding target site in the TGF-β sequence. The sequences of the TGF-β mRNA 3'-UTR

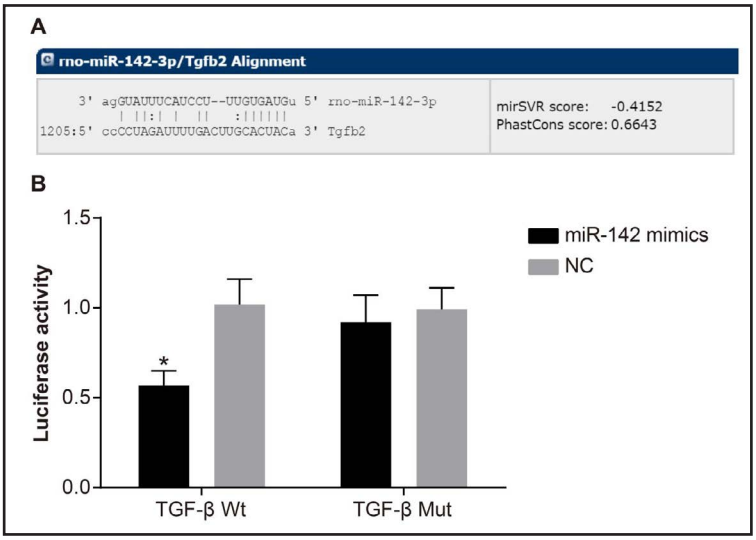

Fig. 5. MiR-142 directly targets TGF-β Notes: A, miR-142 was combined with TGF-β 3'UTR; B, luciferase activity was detected using a dual luciferase reporter gene assay, and miR-142 mimics inhibited the luciferase activity of the wt plasmid; * refers to P<0.05, but no change was observed in the activity of the mut plasmid fluorescent enzyme; the experiment was repeated 3 times; TGF-β, transforming growth factor-β; UTR, untranslated regions; NC, negative control.

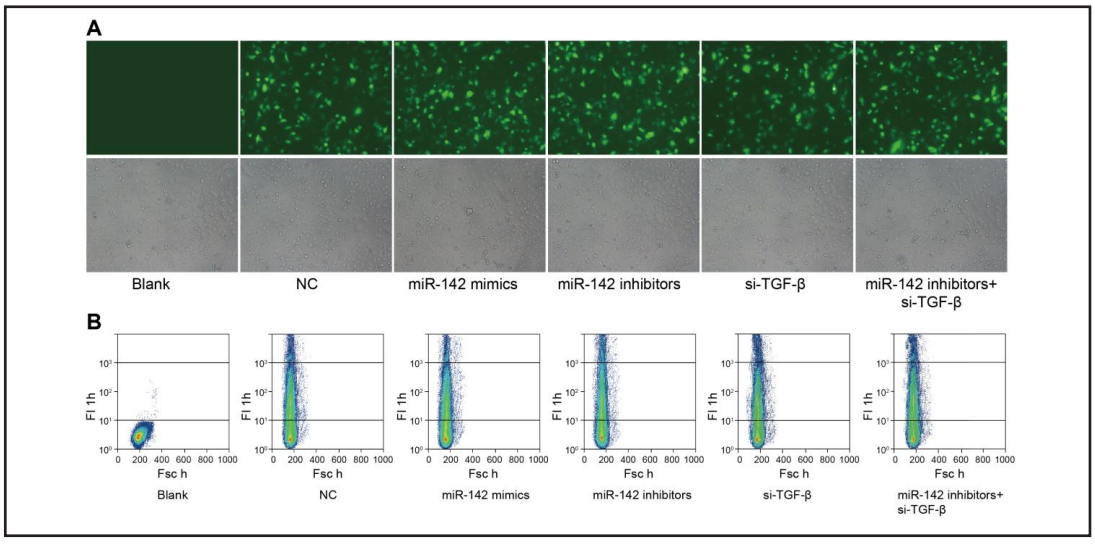

Fig. 6. Transfection efficiency of cells in each group according to immunofluorescence and flow cytometry Notes: A, transfection efficiency of cells in each group according to immunofluorescence; B, transfection efficiency of cells in each group according to flow cytometry; NC, negative control.

region and miR-142 are shown in Fig. 5A. To verify that miR-142 exerted its function at the predicted binding site, we used a luciferase assay. Mutant (containing an miR-142 binding site deletion) and wild-type (wt) sequences of the TGFβ-3'UTR were designed and inserted into reporter plasmids. A luciferase activity assay was performed, and miR-142 mimics were co-transfected into ASMCs with wt-miR-142/TGF-β or mutant (mut-miR-142/TGF-β) recombinant plasmids. The results showed that while the miR-142 mimics had no significant effect on the luciferase activity of Mut-miR-142/TGF-β ($P > 0.05$), the mimics reduced the luciferase activity intensity of wt-miR-142/TGF-β by approximately 44.1% ($P < 0.05$) (Fig. 5B).

Expression levels of miR-142 and TGF-β in transfected cells from each group

ASMC transfection efficiency was evaluated under a fluorescence microscope. Green fluorescence was observed in experimental groups and compared with the blank group (Fig. 6). The transfection efficiency in these cells was greater than 98%. The flow cytometry results showed green fluorescence in all transfected groups, with transfection efficiency as high as

81%. These results indicated that these reagents were appropriate for use in subsequent experiments.

The expression level of miR-142 in the transfected cells in each group is shown in Fig. 7A. miR-142 was significantly upregulated in ASMCs in the miR-142 mimics group but significantly downregulated in the miR-142 inhibitors group and the miR-142 inhibitors + si-TGF-β group (all P < 0.05). There was no significant difference in the expression of miR-142 between the control and the si-TGF-β group (P > 0.05). TGF-β mRNA and protein expression levels showed similar trends in the transfected cells from each group (Fig. 7A-C). The TGF-β expression level was significantly lower in the miR-142 mimics group and the si-TGF-β group than that in the blank group and was significantly higher in the miR-142 inhibitors group than that in the blank group (all P < 0.05). There was no significant difference in the expression of TGF-β between the blank group and the miR-142 inhibitors + si-TGF-β group (P > 0.05).

Upregulation of miR-142 and downregulation of TGF-β blocked ASMC proliferation

MTT assays (Fig. 8) showed that after 24 h, there was no significant difference in OD values, which reflect cell viability, among the ASMCs in each group (all P > 0.05). There was no significant difference in cell viability among ASMCs in the blank group, the NC group or the miR-142 inhibitors + si-TGF-β group at any of the three analyzed time points (all P > 0.05). At 48 h and 72 h, cell viability was significantly higher in the miR-142 inhibitors group but significantly lower in the miR-142 mimics group and si-TGF-β group compared with that in the blank group (all P < 0.05). Additionally, at 48 h and 72 h, the proliferation

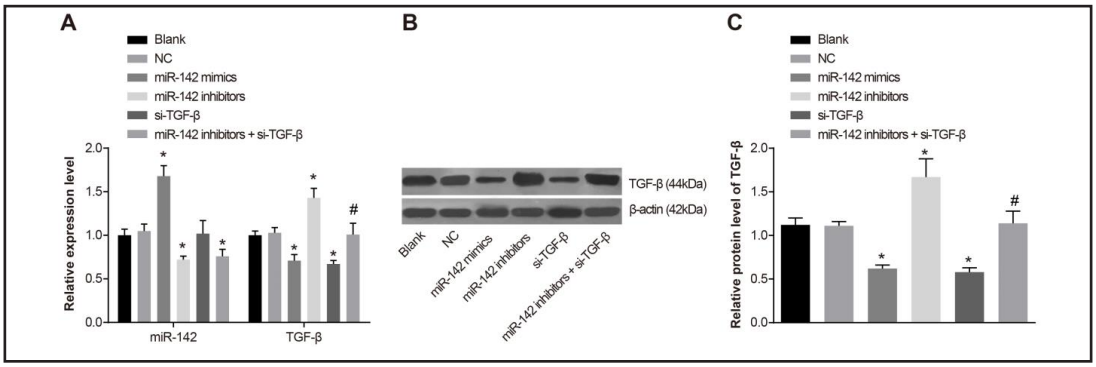

Fig. 7. Expression levels of miR-142 and TGF-β and the correlation between miR-142 and TGF-β in the transfected cells. Notes: A, histogram of miR-142 expression and the mRNA expression of TGF-β in cells in each group; B, western blotting analysis of the protein expression of TGF-β in cells in each group; C, histogram of the protein expression level of TGF-β in each group; *, compared to the blank group and NC group, P<0.05; #, compared to the miR-142 inhibitors group, P<0.05; the experiment was repeated 3 times; miRNA-142, microRNA-142; TGF-β, transforming growth factor-β; NC, negative control.

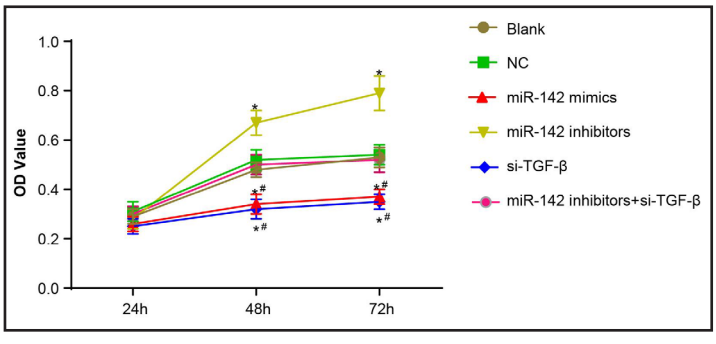

Fig. 8. Line chart showing the proliferation rates of the transfected cells in each group. Notes: miR-142 significantly inhibited cell viability; miR-142 mimics significantly promoted cell viability; *, compared to the blank group and NC group, P<0.05; #, compared to the miR-142 inhibitors group, P<0.05; NC, negative control; the experiment was repeated 3 times.

rate was notably lower in the miR-142 inhibitors + si-TGF-β group than that in the miR-142 inhibitors group (all P < 0.05). Results obtained indicated that upregulation of miR-142 and downregulation of TGF-β blocked proliferation in ASMCs.

Upregulation of miR-142 and downregulation of TGF-β arrested more ASMC in G1 phase and less ASMCs in S phase

The PI single-staining analysis (Fig. 9) showed no significant difference in cell cycle stage distribution among the blank, NC and miR-142 inhibitors + si-TGF-β groups (all P > 0.05). In contrast, the percentage of cells in the G1 phase was significantly lower while the

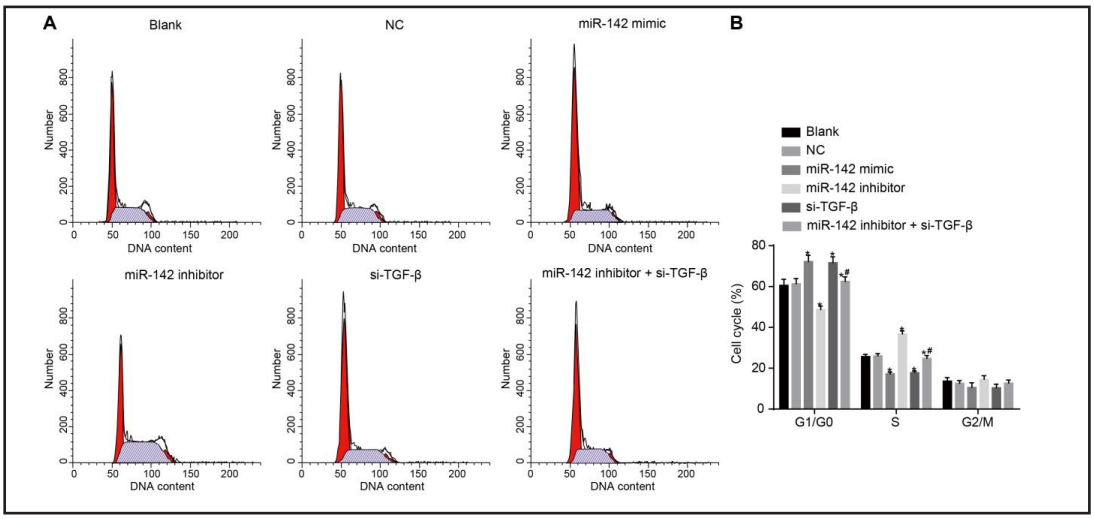

Fig. 9. Analysis of the cell cycle in the transfected cells in each group according to PI single staining. Notes: A, results of an analysis of the cell cycle in each group according to PI single staining; B, histogram of a ratio analysis of the distribution of cells in the cell cycle in each group; *, compared to the blank group and NC group, P<0.05; #, compared to the miR-142 inhibitors group, P<0.05; the experiment was repeated 3 times; in the red region, the first peak represents G1 phase, and the second peak indicates the G2 and S phases; PI, propidium iodide; NC, negative control.

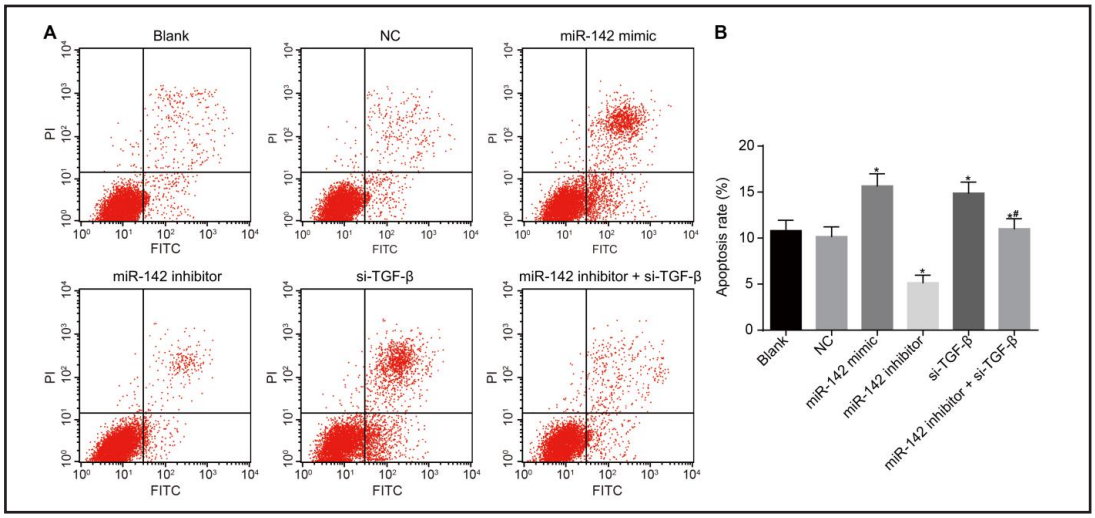

Fig. 10. Cell apoptosis was analyzed at 48 h after transfection in each group using Annexin V/PI double staining.Notes: A, cell apoptosis was detected using flow cytometry; B, histogram showing the cell apoptosis rate in each group; *, compared to the blank group and NC group, P<0.05; #, compared to the miR-142 inhibitors group, P<0.05; NC, negative control; the experiment was repeated 3 times.

percentage in the S phase was significantly higher (both P < 0.05) in the miR-142 inhibitors group compared with those in the blank group. These results indicated that the number of ASMCs undergoing mitosis increased in the model group. The percentage of cells in the G1 phase was higher, while the percentage in the S phase was lower in the miR-142 mimics and si-TGF-β groups than those in the blank group (P < 0.05). ASMC proliferation was correspondingly significantly inhibited in these groups. The percentage of cells in the G1 phase was higher while the percentage in the S phase was lower in the miR-142 inhibitors + si-TGF-β group compared with those in the miR-142 inhibitors group (all P < 0.05), based on which, we could demonstrate that upregulation of miR-142 and downregulation of TGF-β arrested more ASMCs in G1 phase and less ASMCs in S phase.

Upregulation of miR-142 and downregulation of TGF-β promoted apoptosis in ASMCs

The Annexin V/PI double staining (Fig. 10) showed no significant difference in the apoptosis rate of ASMCs among the blank, NC group and miR-142 inhibitors + si-TGF-β groups (all P > 0.05). ASMC apoptosis rate was significantly elevated in the miR-142 mimics group, the si-TGF-β group, and the miRNA-142 inhibitors group compared with that in the blank group (all P < 0.05). Finally, the apoptosis rate in ASMCs was markedly higher in the miR-142 inhibitors + si-TGF-β group than that in the miR-142 inhibitors group (P < 0.05). These findings revealed that upregulation of miR-142 and downregulation of TGF-β promoted apoptosis in ASMCs.

Upregulation of miR-142 and downregulation of TGF-β inhibited the expression of EGFR signaling pathway-related proteins and promoted the expression of apoptosis -related proteins

Western blot analysis (Fig. 11) showed no significant difference in the expression of apoptosis- or EGFR pathway-related proteins among the NC, blank and miR-142 inhibitors + si-TGF-β groups (all P > 0.05). The expression levels of TGF-β, EGFR, Akt, p-Akt, Bcl-2 and Bcl-xl were significantly lower while the expression of P21 and Bax were significantly higher in the miR-142 mimics and si-TGF-β groups than those in the blank group (all P < 0.05). Additionally, the expression levels of TGF-β, EGFR, Akt, p-Akt, Bcl-2 and Bcl-xl were significantly higher while the expression levels of p21 and Bax were significantly lower

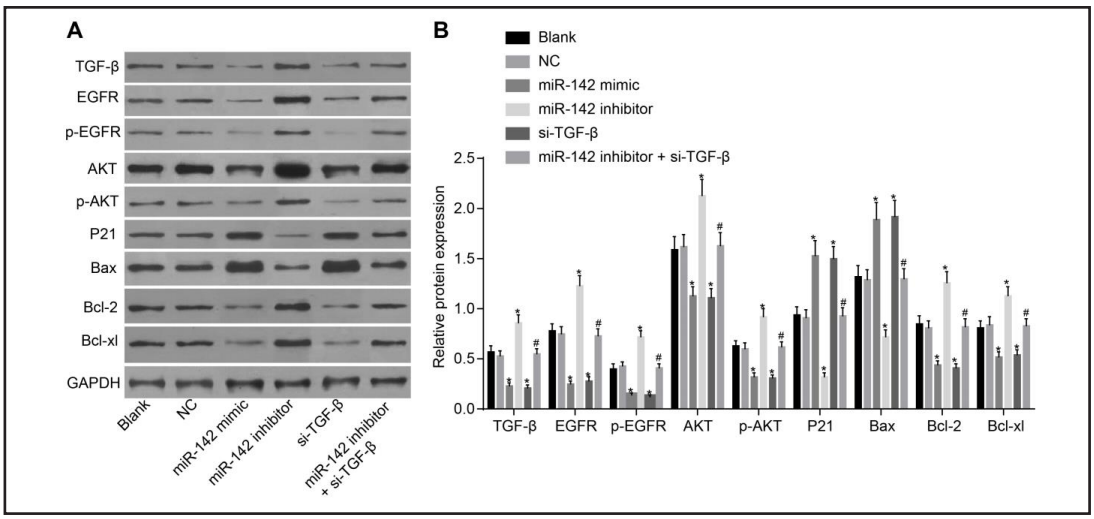

Fig. 11. Changes in cell proliferation, the cycle and apoptosis and EGFR signaling pathway-related proteins in each group. Notes: A, expression levels of protein markers of cell proliferation, the cell cycle, apoptosis and the EGFR signaling pathway according to western blotting; B, histograms showing the protein expression of markers of cell proliferation, the cell cycle, apoptosis and the EGFR signaling pathway; *, compared to the blank group and NC group, P<0.05; #, compared to the miR-142 inhibitors group, P<0.05; NC, negative control; the experiment was repeated 3 times.

in the miR-142 inhibitors group than those in the blank group (all $P < 0.05$). Finally, the expression levels of TGF-β, EGFR, Akt, p-Akt, Bcl-2 and Bcl-xl were significantly lower while the expression levels of P21 and Bax were significantly increased in the miR-142 inhibitors + si-TGF-β group compared with those in the miR-142 inhibitors group (all $P < 0.05$). It was suggested that upregulation of miR-142 and downregulation of TGF-β inhibited the expression of EGFR signaling pathway-related proteins and promoted the expression of apoptosis-related proteins.

Discussion

Airway remodeling is defined as the deposition of collagen and associated structural changes in an asthmatic airway, including smooth-muscle hypertrophy and cell hyperplasia [17, 18]. Because airway remodeling represents a significant social and economic burden, asthma has become an important health challenge in developed countries [19]. A recent study had revealed that some angiogenic and inflammatory signal pathways, such as FGFR, are involved in both pulmonary diseases and cancer [20]. Thus, studies exploring potential regulators of airway remodeling and ASMC physiology are crucial for identifying potential targets for the treatment of asthma.

By utilizing a rat experimental of chronic asthma, we were able to show an association between miR-142 and asthma. Expression levels of several miRNAs have been implicated in asthma and airway inflammation. These include miR-21, miR-223, and especially miR-142-3p [21]. Additionally, miR-203 expression negatively regulates ASMC proliferation, while miR-221 inhibits ASMC hyperproliferation in asthma patients [22]. Moreover, miR-26a plays a regulatory role in ASMC hypertrophy, which is a crucial process in the development of airway remodeling [23]. It was previously reported that miR-142-3p is associated with differentiation and proliferation of mesenchymal units [24] and that epithelial-mesenchymal units affect asthma [17]. A previous study indicated that miR-142-3p plays a significant role in maintaining the self-renewal capacity of broncho-alveolar stem cells (BASCs) [25]. In this study, we show that miR-142 influences airway remodeling and ASMC proliferation and is therefore involved in the development of asthma. Furthermore, we show that our rat asthma models exhibited reduced miR-142 expression. Relatedly, Jiang et al. reported that miR-142 was expressed at low levels in several cancer tissues and was associated with pathological indicators in cancer patients; miR-142 overexpression was also found to influence prostate cancer cell growth by targeting the androgen receptor [26]. However, few studies have investigated the dynamics of miR-142 expression or the mechanism by which miR-142 exerts its effects. The mechanisms underlying the activity of miR-142 therefore need to be further characterized.

In this study, we focused on the relationship between miR-142 and the TGF-β/EGFR signaling pathway. We found that in asthmatic rats, inhibition of TGF-β miR-142 influenced airway remodeling and ASMC proliferation, and we showed that miR-142 may also inhibit the EGFR signaling pathway to alter cell cycle- and apoptosis-related proteins. TGF-β has two receptors that participate in signal transmission. These are TGF-β receptor 1 (TGFβR1), which is potentially targeted by miR-142-3p, and TGF-β receptor 2 (TGFβR2) [25]. TGF-β is a multifunctional growth factor involved in cellular development, differentiation and proliferation [27]. TGF-β may induce epithelial cell apoptosis or anti-apoptotic action in asthmatic airways depending on context, and it plays a role in enhancing ASMC proliferation via its effects on the mitogen-activated protein kinase (MAPK) pathway [2]. miR-142-3p has been shown to influence the TGF-β signaling pathway in both Raji and B cells [28], and another study suggested that miR-142-3p and miR-142-3p_-1_5 may suppress the TGF-β signaling pathway [29]. One study demonstrated that miR-142-3p impaired TGF-β signaling by targeting TGF-β and promoted cell proliferation by repressing TGF-βR1 [25] In asthma, EGFR plays a key role in airway remodeling and tissue repair [30]. The increased expression of EGFR is a feature of epithelial alterations in the asthmatic airway, and epithelial EGFR

activation results in several important features of asthma [31]. There is also evidence that increased EGFR levels are related to the severity of airway thickening in patients with chronic asthma, which is induced by asthma-related inflammation as well as cytokines [32]. A previous study showed that miR-125a-5p is potentially regulated by activated EGFR signaling and could be involved in the inhibition of metabolism [33]. Our study found that miR-142 targeted TGF-β and that miR-142 was negatively associated with TGF-β expression. We also showed that miR-142 changes the rates of cellular apoptosis and proliferation and that components of the EGFR signaling pathway are downregulated by miR-142. Therefore, the results of this study indicate that miR-142 targets TGF-β to inactivate the EGFR signaling pathway, which itself regulates ASMC proliferation in asthmatic rats.

In conclusion, the results of our study indicate that miR-142 inhibits proliferation and promotes apoptosis in ASMCs during airway remodeling in asthmatic rats by inhibiting the expression of TGF-β and related proteins in the EGFR signaling pathway. Further analysis of the molecular mechanisms underlying airway remodeling is required for the development of new therapeutic strategies for asthma. Future studies that include larger sample sizes are needed to determine the specific mechanism by which miR-142 exerts its effects.

Acknowledgements

We would like to thank all the participants who enrolled in the present study.

Disclosure Statement

All the authors declare that they have no conflicts of interest.

References

1 Shifren A, Witt C, Christie C, Castro M: Mechanisms of remodeling in asthmatic airways. J Allergy (Cairo) 2012;2012:316049.
2 Halwani R, Al-Muhsen S, Al-Jahdali H, Hamid Q: Role of transforming growth factor-beta in airway remodeling in asthma. Am J Respir Cell Mol Biol 2011;44:127-133.
3 Postma DS, Timens W: Remodeling in asthma and chronic obstructive pulmonary disease. Proc Am Thorac Soc 2006;3:434-439.
4 Vignola AM, Mirabella F, Costanzo G, Di Giorgi R, Gjomarkaj M, Bellia V, Bonsignore G: Airway remodeling in asthma. Chest 2003;123:417S-422S.
5 Homer RJ, Elias JA: Airway remodeling in asthma: Therapeutic implications of mechanisms. Physiology (Bethesda) 2005;20:28-35.
6 Wei Y, Xu YD, Yin LM, Wang Y, Ran J, Liu Q, Ma ZF, Liu YY, Yang YQ: Recombinant rat cc10 protein inhibits pdgf-induced airway smooth muscle cells proliferation and migration. Biomed Res Int 2013;2013:690937.
7 Anandan C, Nurmatov U, van Schayck OC, Sheikh A: Is the prevalence of asthma declining? Systematic review of epidemiological studies. Allergy 2010;65:152-167.
8 Krol J, Loedige I, Filipowicz W: The widespread regulation of microrna biogenesis, function and decay. Nat Rev Genet 2010;11:597-610.
9 Sharma S, Liu J, Wei J, Yuan H, Zhang T, Bishopric NH: Repression of mir-142 by p300 and mapk is required for survival signalling via gp130 during adaptive hypertrophy. EMBO Mol Med 2012;4:617-632.
10 Ma Z, Liu T, Huang W, Liu H, Zhang HM, Li Q, Chen Z, Guo AY: Microrna regulatory pathway analysis identifies mir-142-5p as a negative regulator of tgf-beta pathway via targeting smad3. Oncotarget 2016;7:71504-71513.
11 Chanda S, Nandi S, Chawla-Sarkar M: Rotavirus-induced mir-142-5p elicits proviral milieu by targeting non-canonical transforming growth factor beta signalling and apoptosis in cells. Cell Microbiol 2016;18:733-747.

12 Kim K, Yang DK, Kim S, Kang H: Mir-142-3p is a regulator of the tgfbeta-mediated vascular smooth muscle cell phenotype. J Cell Biochem 2015;116:2325-2333.
13 Li XZ, Feng JT, Hu CP, Chen ZQ, Gu QH, Nie HP: Effects of arkadia on airway remodeling through enhancing tgf-beta signaling in allergic rats. Lab Invest 2010;90:997-1003.
14 Terakado M, Gon Y, Sekiyama A, Takeshita I, Kozu Y, Matsumoto K, Takahashi N, Hashimoto S: The rac1/jnk pathway is critical for egfr-dependent barrier formation in human airway epithelial cells. Am J Physiol Lung Cell Mol Physiol 2011;300:L56-63.
15 Burgel PR, Nadel JA: Roles of epidermal growth factor receptor activation in epithelial cell repair and mucin production in airway epithelium. Thorax 2004;59:992-996.
16 Xu YD, Wei Y, Wang Y, Yin LM, Park GH, Liu YY, Yang YQ: Exogenous s100a8 protein inhibits pdgf-induced migration of airway smooth muscle cells in a rage-dependent manner. Biochem Biophys Res Commun 2016;472:243-249.
17 Grainge CL, Lau LC, Ward JA, Dulay V, Lahiff G, Wilson S, Holgate S, Davies DE, Howarth PH: Effect of bronchoconstriction on airway remodeling in asthma. N Engl J Med 2011;364:2006-2015.
18 Hong W, Peng G, Hao B, Liao B, Zhao Z, Zhou Y, Peng F, Ye X, Huang L, Zheng M, Pu J, Liang C, Yi E, Peng H, Li B, Ran P: Nicotine-induced airway smooth muscle cell proliferation involves trpc6-dependent calcium influx via alpha7 nachr. Cell Physiol Biochem 2017;43:986-1002.
19 Wenzel SE: Asthma phenotypes: The evolution from clinical to molecular approaches. Nat Med 2012;18:716-725.
20 Tan H, Lei J, Xue L, Cai C, Liu QH, Shen J: Relaxing effect of tsu-68, an antiangiogenic agent, on mouse airway smooth muscle. Cell Physiol Biochem 2017;41:2350-2362.
21 Jiang X: The emerging role of micrornas in asthma. Mol Cell Biochem 2011;353:35-40.
22 Sun M, Lu Q: Microrna regulation of airway smooth muscle function. Biol Chem 2016;397 (6):507-511.
23 Mohamed JS, Lopez MA, Boriek AM: Mechanical stretch up-regulates microrna-26a and induces human airway smooth muscle hypertrophy by suppressing glycogen synthase kinase-3beta. J Biol Chem 2010;285:29336-29347.
24 Carraro G, Shrestha A, Rostkovius J, Contreras A, Chao CM, El Agha E, Mackenzie B, Dilai S, Guidolin D, Taketo MM, Gunther A, Kumar ME, Seeger W, De Langhe S, Barreto G, Bellusci S: Mir-142-3p balances proliferation and differentiation of mesenchymal cells during lung development. Development 2014;141:1272-1281.
25 Lei Z, Xu G, Wang L, Yang H, Liu X, Zhao J, Zhang HT: Mir-142-3p represses tgf-beta-induced growth inhibition through repression of tgfbetar1 in non-small cell lung cancer. FASEB J 2014;28:2696-2704.
26 Jiang D, Wang H, Li Z, Li Z, Chen X, Cai H: Mir-142 inhibits the development of cervical cancer by targeting hmgb1. Oncotarget 2017;8:4001-4007.
27 Takeda H, Inoue H, Kutsuna T, Matsushita N, Takahashi T, Watanabe S, Higashiyama S, Yamamoto H: Activation of epidermal growth factor receptor gene is involved in transforming growth factor-beta-mediated fibronectin expression in a chondrocyte progenitor cell line. Int J Mol Med 2010;25:593-600.
28 Danger R, Pallier A, Giral M, Martinez-Llordella M, Lozano JJ, Degauque N, Sanchez-Fueyo A, Soulillou JP, Brouard S: Upregulation of mir-142-3p in peripheral blood mononuclear cells of operationally tolerant patients with a renal transplant. J Am Soc Nephrol 2012;23:597-606.
29 Lei X, Zhu Y, Jones T, Bai Z, Huang Y, Gao SJ: A kaposi's sarcoma-associated herpesvirus microrna and its variants target the transforming growth factor beta pathway to promote cell survival. J Virol 2012;86:11698-11711.
30 Hirota N, Risse PA, Novali M, McGovern T, Al-Alwan L, McCuaig S, Proud D, Hayden P, Hamid Q, Martin JG: Histamine may induce airway remodeling through release of epidermal growth factor receptor ligands from bronchial epithelial cells. FASEB J 2012;26:1704-1716.
31 Habibovic A, Hristova M, Heppner DE, Danyal K, Ather JL, Janssen-Heininger YM, Irvin CG, Poynter ME, Lundblad LK, Dixon AE, Geiszt M, van der Vliet A: Duox1 mediates persistent epithelial egfr activation, mucous cell metaplasia, and airway remodeling during allergic asthma. JCI Insight 2016;1:e88811.
32 Song L, Tang H, Liu D, Song J, Wu Y, Qu S, Li Y: The chronic and short-term effects of gefinitib on airway remodeling and inflammation in a mouse model of asthma. Cell Physiol Biochem 2016;38:194-206.
33 Wang G, Mao W, Zheng S, Ye J: Epidermal growth factor receptor-regulated mir-125a-5p--a metastatic inhibitor of lung cancer. FEBS J 2009;276:5571-5578.

MicroRNA-142 Inhibits Proliferation and Promotes Apoptosis in Airway Smooth Muscle Cells During Airway Remodeling in Asthmatic Rats via -Dependent EGFR

- Cell Physiol Biochem 2018;47:1682-1695 - DOI: 10.1159/000490236

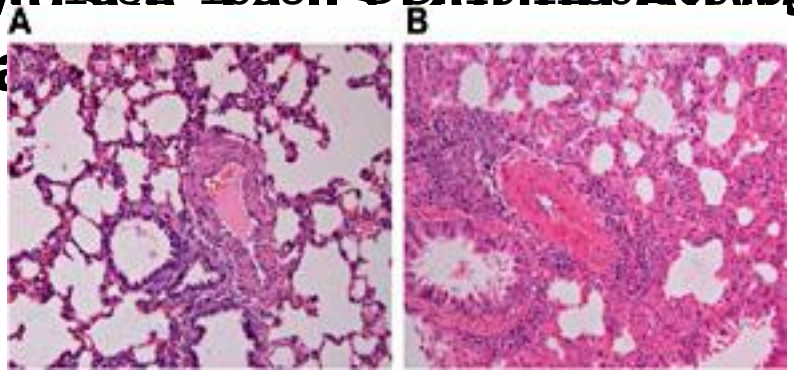

- © 2018 The Author(s). Published by S. Karger AG, Basel - CC BY-NC-ND 4.0

MicroRNA-142 Inhibits Proliferation and Promotes Apoptosis i Airway Smooth Muscle Cells During Airway Remodeling in Asthmatic Rats via -Dependent EGFR

• Cell Physiol Biochem 2018;47:1682-1695 - DOI: 10.1159/000490236

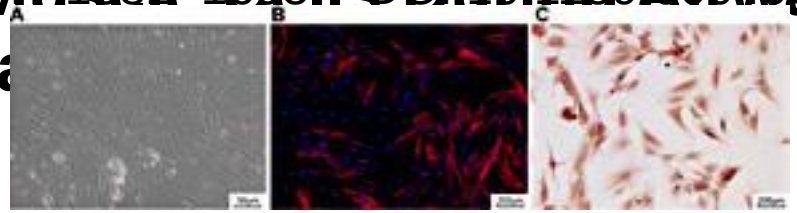

• © 2018 The Author(s). Published by S. Karger AG, Basel - CC BY-NC-ND 4.0

MicroRNA-142 Inhibits Proliferation and Promotes Apoptosis in Airway Smooth Muscle Cells During Airway Remodeling in Asthmatic Rats via Cell-Dependent EGFR

• Cell Physiol Biochem 2018;47:1682-1695 - DOI: 10.1159/000490236

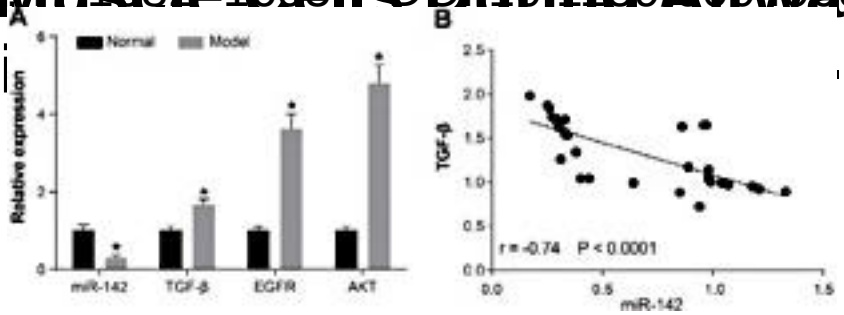

• © 2018 The Author(s). Published by S. Karger AG, Basel - CC BY-NC-ND 4.0

MicroRNA-142 Inhibits Proliferation and Promotes Apoptosis in Airway Smooth Muscle Cells During Airway Remodeling in Asthmatic Rats via the Inhibition of TGF-β -Dependent EGFR Signaling Pathway

- Cell Physiol Biochem 2018;47:1682-1695 - DOI: 10.1159/000490236

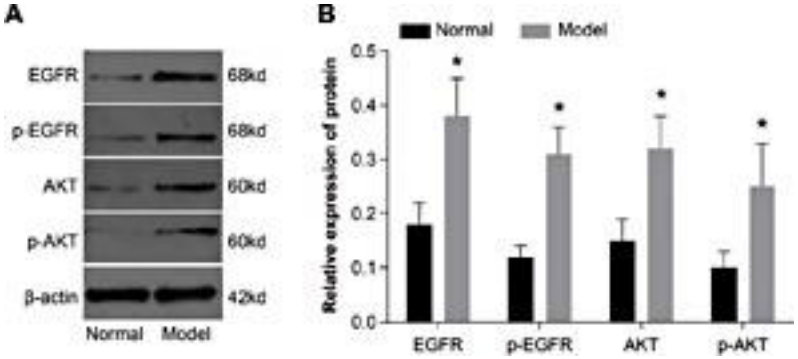

- © 2018 The Author(s). Published by S. Karger AG, Basel - CC BY-NC-ND 4.0

MicroRNA-142 Inhibits Proliferation and Promotes Apoptosis i Airway Smooth Muscle Cells During Airway Remodeling in Asthmatic Rats: pendent EGFR

• Cell Physiol Biochem 2018;47:1682-1695 - DOI: 10.1159/000490236

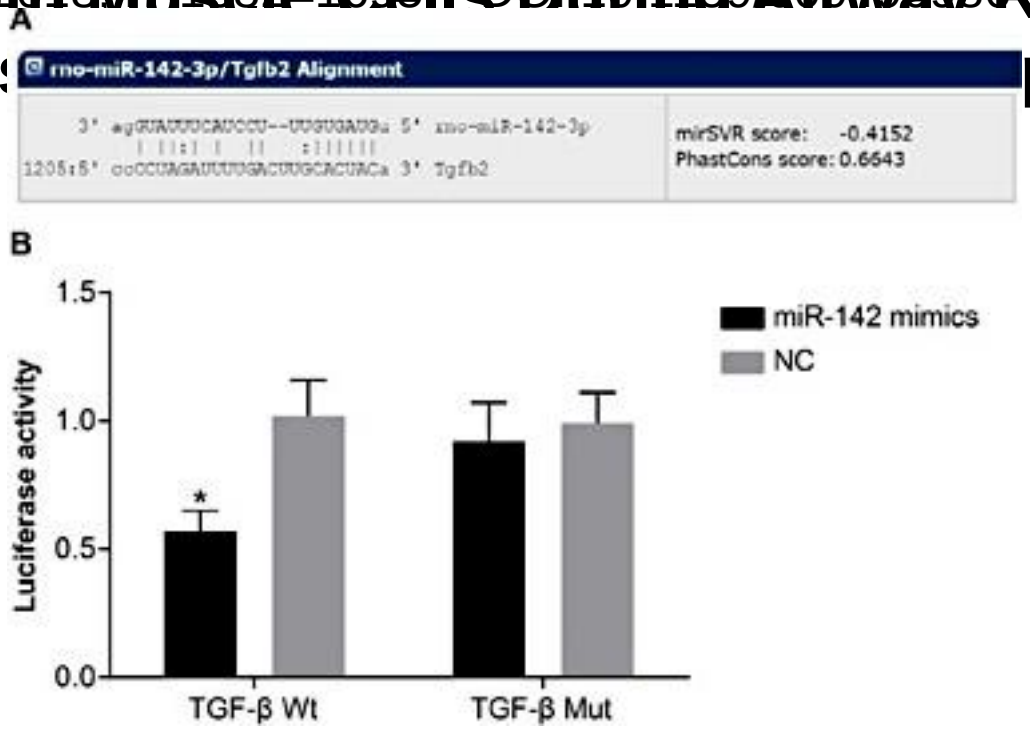

• © 2018 The Author(s). Published by S. Karger AG, Basel - CC BY-NC-ND 4.0

MicroRNA-142 Inhibits Proliferation and Promotes Apoptosis i Airway Smooth Muscle Cells During Airway Remodeling in Asthmatic ent EGFR

• Cell Physiol Biochem 2018;47:1682-1695 - DOI: 10.1159/000490328

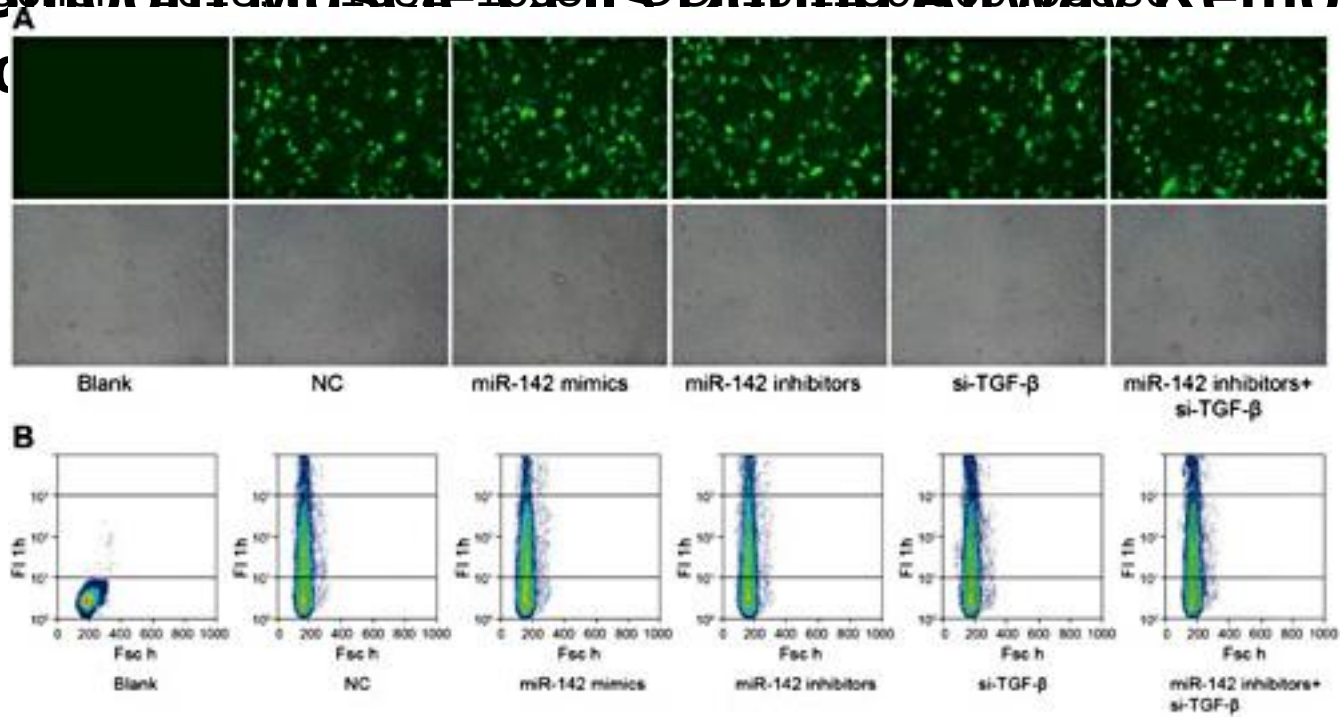

• © 2018 The Author(s). Published by S. Karger AG, Basel - CC BY-NC-ND 4.0

MicroRNA-142 Inhibits Proliferation and Promotes Apoptosis i Airway Smooth Muscle Cells During Airway Remodeling in Asthmat nt EGFR

- Cell Physiol Biochem 2018;47:1682-1695 - DOI: 10.1159/000490328

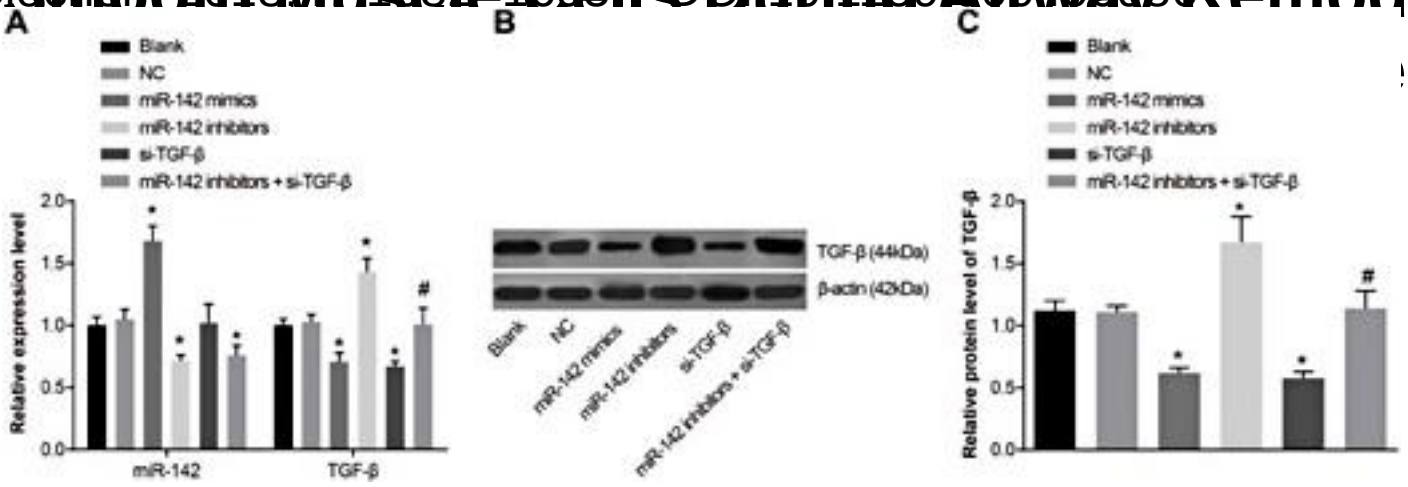

- © 2018 The Author(s). Published by S. Karger AG, Basel - CC BY-NC-ND 4.0

MicroRNA-142 Inhibits Proliferation and Promotes Apoptosis i Airway Smooth Muscle Cells Induced Airway Remodeling in Asthmatic Rats ependent EGFR

• Cell Physiol Biochem 2018;47:1682-1695 - DOI: 10.1159/000490236

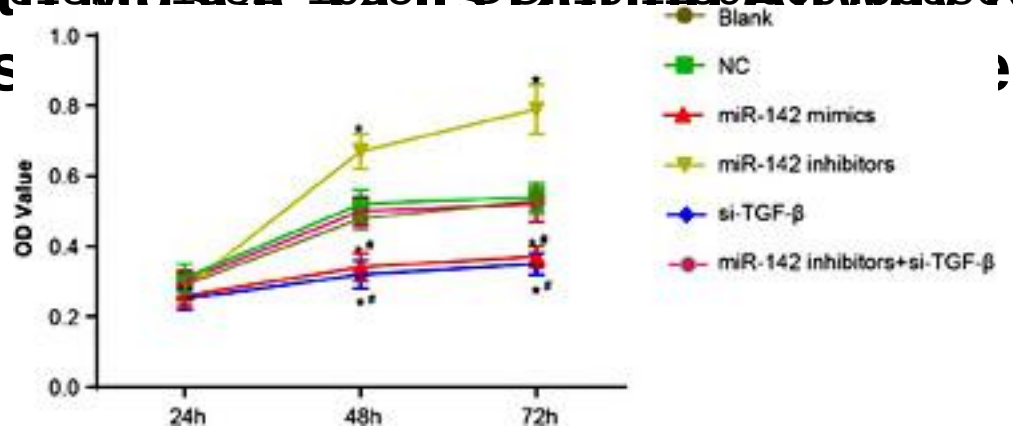

• © 2018 The Author(s). Published by S. Karger AG, Basel - CC BY-NC-ND 4.0

MicroRNA-142 Inhibits Proliferation and Promotes Apoptosis i Airway Smooth Muscle Cells During Airway Remodeling in Asthmat nt EGFR

• Cell Physiol Biochem 2018;47:1682-1695 - DOI: 10.1159/000490328

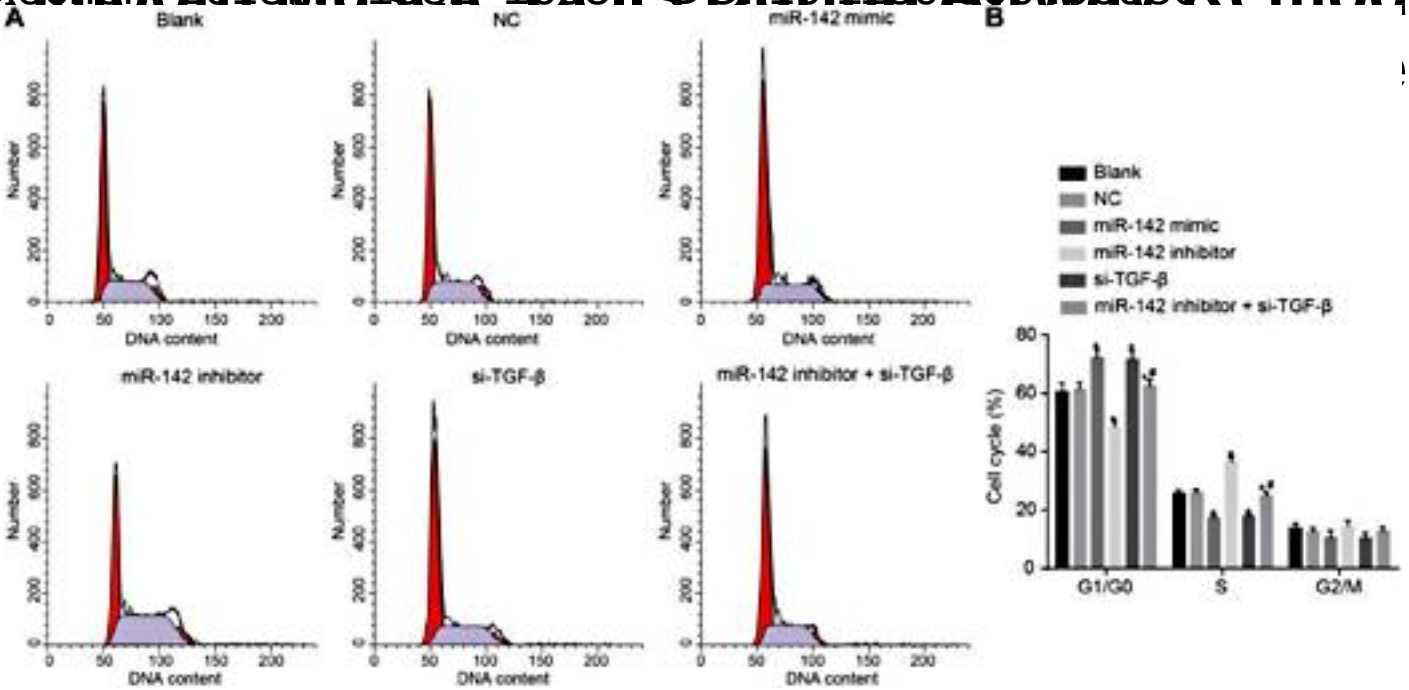

• © 2018 The Author(s). Published by S. Karger AG, Basel - CC BY-NC-ND 4.0

MicroRNA-142 Inhibits Proliferation and Promotes Apoptosis i
Airway Smooth Muscle Cells During Airway Remodeling in
Asthmat nt EGFR

• Cell Physiol Biochem 2018;47:1682-1695 - DOI:10.1159/000490986

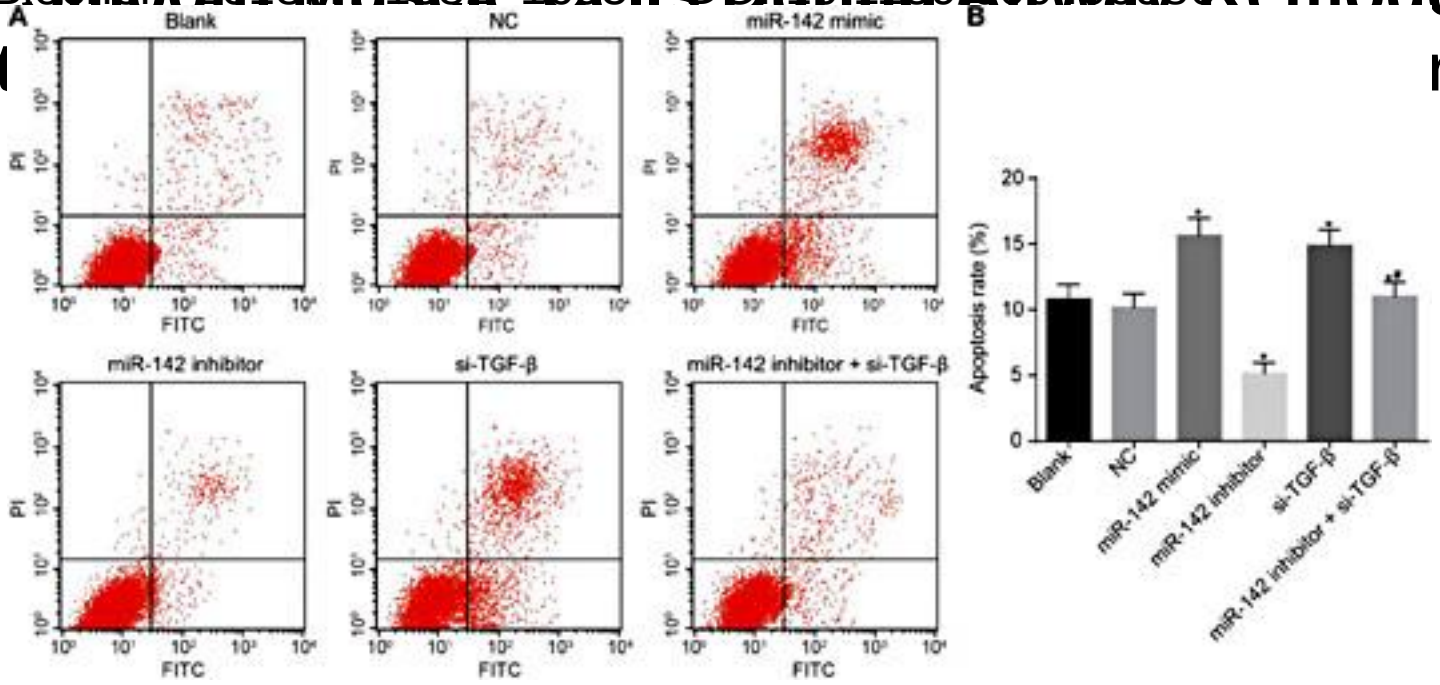

• © 2018 The Author(s). Published by S. Karger AG, Basel - CC BY-NC-ND 4.0

MicroRNA-142 Inhibits Proliferation and Promotes Apoptosis i Airway Smooth Muscle Cells During Airway Remodeling in Asthmati ent EGFR

• Cell Physiol Biochem 2018;47:1682-1695 - DOI: 10.1159/000490328

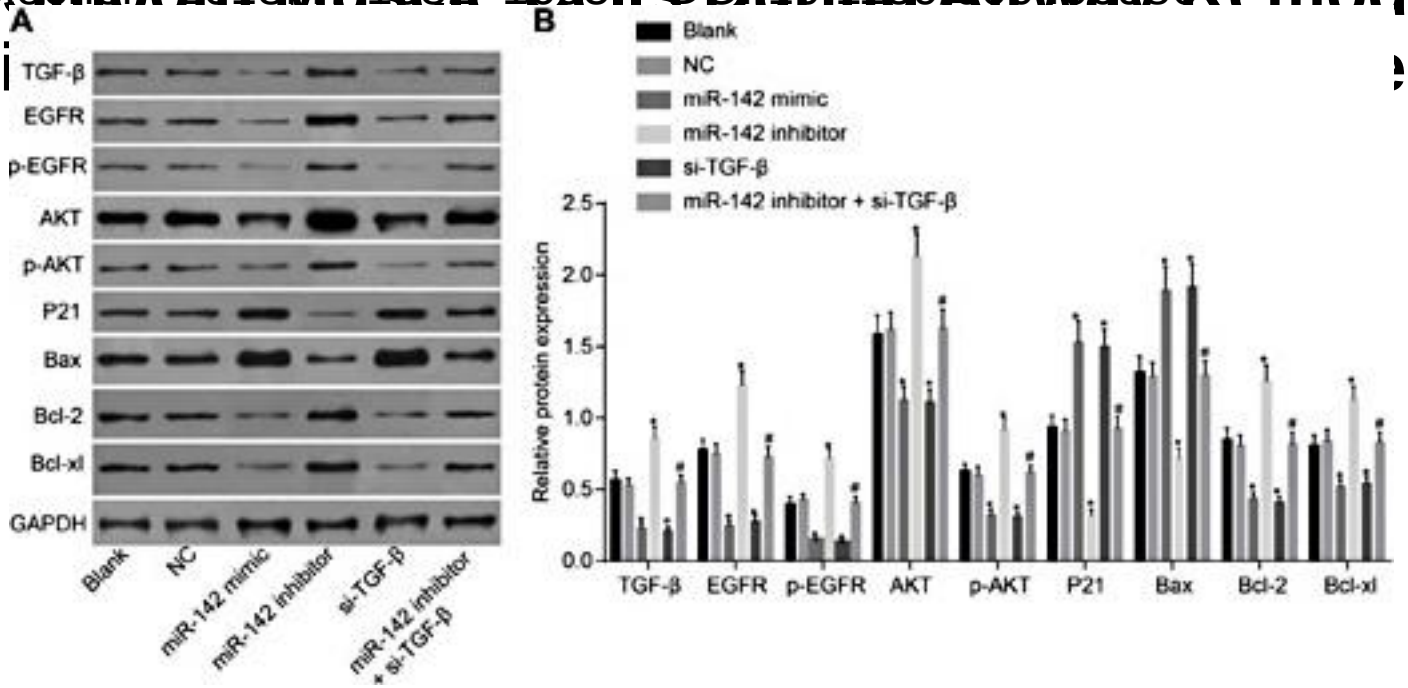

• © 2018 The Author(s). Published by S. Karger AG, Basel - CC BY-NC-ND 4.0

(μm2/μm2)	S/Pi (μm2/
1 ± 0.95	1.30 ± 0.
± 0.88*	2.75 ± 0.5

Primer Sequences
Forward 5'-GTGACCTGTAGTGTT
Reverse 5'-TATGGTTGTTCTGCTC
Forward 5'-ATTGGAACGATACAG
Reverse 5'-GGAACGCTTCACG
Forward 5'-ACTGATACGCCTGA
Reverse 5'-CTCTGTGGAGCTGA
Forward 5'-ACC GGC AGG ATG T
Reverse 5'-GGC CGA CAG CTA TG
erward 5'--GGGCTAGCGATGAGCGAC
Reverse 5'-GGGGTACCGGGCCTGCCGC
Forward 5'-CGTACGTGACATT
Reverse 5'-TTGCCGATAGTGA